E2F-1-Deficient NOD/SCID Mice Developed Showing Decreased Saliva Production

Hikaru Matsui-Inohara,*,† Hiroshi Uematsu,* Takanori Narita,‡ Keitaro Satoh,‡ Hideo Yonezawa,§ Koichiro Kuroda,|| Tatsuro Ito,† Saori Yoneda,† Taketo Kawarai,† Hiroshi Sugiya,‡ Haruo Watanabe,† and Hidenobu Senpuku†,[1]

*Department of Gerodontology, Graduate School, Tokyo Medical and Dental University, Tokyo 113-8549, Japan; †Department of Bacteriology, National Institute of Infectious Diseases, Tokyo 162-8640, Japan; ‡Department of Physiology, Nihon University School of Dentistry at Matsudo, Chiba 271-8587, Japan; §Division of Medical Microbiology, Department of Infectious Diseases, Kyorin University School of Medicine, Tokyo 181-8611, Japan; and ||Department of Bacteriology, Nihon University School of Dentistry, Tokyo 101-8310, Japan

The non-obese diabetic mouse (NOD) is the most characterized model used to study insulin-dependent type 1 diabetes mellitus (IDDM) and Sjögren's syndrome (SS). In a previous report, we found NOD.*E2f1*$^{-/-}$ mice show a greater progressive development to IDDM and SS compared to NOD mice. Our previous data indicated a progressive decrease in regulatory T cells ($CD4^+CD25^+$) and a decrease in the systemic secretion systems for insulin, and saliva was associated with the progression of IDDM and SS. Therefore, to define the mechanism of early-onset IDDM SS in E2F-1 deficient NOD mice required further investigation by producing E2F-1 deficient NOD/SCID mice in which the T and B cells do not develop. The purpose here was to analyze the essential function of the E2F-1 molecule in the development of IDDM and SS; and the dysfunction of the pancreas islet and salivary gland in the NOD background using NOD/SCID mice. We produced NOD/SCID.*E2f1*$^{-/-}$ mice using homologous recombination; determined diabetes development; measured saliva and insulin production; and performed a histological analysis. The deficient mice showed a decreasing volume of saliva; no infiltration of lymphocytes into salivary glands; no development of diabetes; and no protein localization of FGFR-2b in the ducts of the salivary gland that regulates submandibular gland proliferation and morphogenesis. Therefore, we considered a deficiency in E2F-1 induces a decrease in regulatory T cells and an increase in auto-reactive T cells; however, the E2F-1 deficiency is not associated with T and B cells-independent dysfunction of pancreatic β cell in insulin secretion. Further, the E2F-1 deficiency is associated with T and B cells-independent dysfunction of the salivary gland exhibits a decrease in saliva production volume. We suggest E2F-1 may be also associated with the differentiation of exocrine cells in the duct where FGFR-2b is expressed in the salivary gland. The E2F-1 deficient NOD/SCID mouse model is useful for showing the development of the salivary gland; and is also useful for various experiments in humanized mice. Exp Biol Med 234:1525–1536, 2009

Key words: E2F-1; NOD/SCID mouse; oral cavity; pancreas; salivary gland

Introduction

The non-obese diabetic mouse strain (NOD) remains the most characterized model used for the study of insulin-dependent type 1 diabetes mellitus (IDDM) (1, 2) and Sjögren's syndrome (SS); and is a complex model for immune dysregulation involving genetics, sensitivity to exogenous factors, and defects in central and peripheral tolerance (3). IDDM and SS are chronic multisystem and autoimmune disorders (4–6) that spontaneously develop in NOD mice at 4–6 months of age (7). The development of IDDM is characterized by the infiltration of T lymphocytes, dendritic cells, and monocytes into the islets of the pancreas as well as the terminal destruction of β cells (7, 8). Sjögren's syndrome is an autoimmune, chronic inflammatory disease that is characterized by focal mononuclear cell infiltration of the exocrine glands accompanied by loss of secretory function associated with oral and ocular dryness (9, 10). Although some genetic loci related to diabetes (*idd*-loci) were found to contribute to inflammatory changes in the

This work was supported in-part by a grant-in-aid for the Development of Scientific Research (15390571, 19659559 and 18592011) from the Ministry of Education, Science, and Culture of Japan; and by a grant from the Ministry of Health, Labor and Welfare (H16-Medical Services-014 and H19-Medical Services-007).

[1] To whom correspondence should be addressed at Department of Bacteriology, National Institute of Infectious Diseases, 1-23-1 Toyama, Shinjuku-ku, Tokyo 162-8640, Japan. E-mail: hsenpuku@nih.go.jp

Received May 26, 2009.
Accepted August 12, 2009.

DOI: 10.3181/0905-RM-173
1535-3702/09/23412-1525$15.00

exocrine glands, it seems that diabetes and SS-like disease can develop independently from each other (11). Diabetes development in NOD mice is restricted to the expression of MHC I-A^{g7} (12); whereas NOD.B10D2 mice show exocrine gland lymphocytic infiltration typical of SS-like disease while diabetes is absent (13). The exchange of the H2 haplotype suggests a different specificity from the spontaneous autoimmune disease such as IDDM or SS.

E2F factors are involved in the regulation of a number of important cellular events: cell cycle progression, apoptosis, and DNA damage. Further, the E2F family contributes to carcinogenesis in many human tumors (14). The E2F family of transcription factors consists of eight members (E2F-1 to 8). E2F-1, E2F-2, and E2F-3a are potent transactivators that can transiently bind and activate E2F target promoters (15–17). E2F-4, E2F-5 and possibly E2F-3b most likely contribute to the repression of cell growth. The most characterized member of the E2F family is E2F-1, which is activated by the cyclin-Cdk-Rb pathway and plays a major role modulating cellular processes in disease (14, 18, 19). In addition to cellular processes, E2F-1 has important roles in the induction of apoptosis (18, 20).

Several recent studies demonstrate that a mutation in the E2F-1 gene of mice causes enhanced T lymphocyte proliferation, leading to testicular atrophy, splenomegaly, salivary gland dysplasia, and other systemic and organ-specific autoimmunity (21–26). However, it is uncertain whether the function of E2F-1 has an influence on the development of IDDM and SS. To address this issue, we generated E2F-1-deficient NOD mice in our previous study (7). E2F-1-deficient NOD mice present a profound decrease in immuno-regulatory $CD4^+CD25^+$ T cells; whereas their splenocytes produced significantly increased levels of IFN-γ in response to antigenic stimulation *in vitro*. Because of these defects, E2F-1 homozygous mutant NOD mice are highly predisposed to the development of IDDM and SS (27). E2F-1 was also required for the maintenance of the endocrine and exocrine compartments (28). The combination of E2F-1 deficiency and the NOD gene background may lead to decreased production of saliva and insulin in addition to enhanced auto-reactive Th1-type T cells. To clarify whether the mechanism involving development of auto-reactive T cells and/or T and B cells-independent dysfunction of the pancreatic β cells and the salivary gland is related with early-onset diabetes and decreased production of saliva, we produced E2F-1-deficient NOD/$Prkdc^{scid/scid}$ (SCID) mice. These mice were generated using homologous recombinations where T and B cells do not develop in order to observe E2F-1 function in the NOD background mice without an auto-reactive response. Further, to test the essential function of the E2F-1 molecule in the mice, we surveyed for diabetes development; measured saliva and insulin production; and performed a histological analysis in NOD/SCID, E2F-1 heterogeneous and homogeneous deficient NOD/SCID mice.

Materials and Methods

Generation of E2F-1-Deficient NOD/SCID Mice.

We previously reported the *E2f1*$^{-/-}$ allele was functionally disrupted using the insertion of a neomycin-resistant gene (neo^R) that had been backcrossed from the original chimeric stock and mixed with the 129/SV and C57BL/6 genome into the NOD inbred N5 backcross generation background (27). To generate the tenth backcross (N11) generation of NOD.*E2f1*$^{-/-}$ mice that are closely related to the NOD background, the NOD.*E2f1*$^{-/-}$ mice BC5 generation (previously reported) were backcrossed with NOD mice to produce backcrosses 6 (BC6), BC7, BC8, BC9, BC10, and BC11. The NOD/SCID mice were originally purchased from Jackson Laboratory (Bar Harbor, ME). To generate NOD/SCID.*E2f1*$^{-/-}$ mice, the N11 generation of NOD.*E2f1*$^{-/-}$ mice were mated with NOD/SCID mice to produce (NOD.*E2f1*$^{-/-}$ mice × NOD/SCID) F1 mice, and then the heterozygous F1 mice were further mated with NOD/SCID mice to produce the first-generation BC1 mice. BC1 mice were surveyed for the absence of mouse IgM in serum and for the presence of neo^R. The BC1 heterozygous mice were then mated with BC1 mice that have neo^R but produce no mouse IgM; thus producing intercross mice. The mice were housed and maintained in polypropylene mouse cages using pine chips. The experimental design was approved in accordance with the guidelines established by the animal office at the National Institute of Infectious Diseases (approval number: 408024). The experiments to produce NOD/SCID.*E2f1*$^{-/-}$ mice were approved by the genetic recombination safety committee at the National Institute of Infectious Diseases (approval number: ki20–31).

PCR. The heterozygous carriers of the *E2f1*$^{-/-}$ allele were used as breeders; and each backcross generation was identified by blood typing the DNA taken from the tail using PCR with the primers (5′-AGGATCTCGTCGTGACCCATGGCGA-3′) and (5′-GAGCGGCGATACCGTAAAGCACGAGG-3′) that generated a 271-bp product from within the neo^R insert. Each amplification cycle was performed using a PTC-200 (MJ Research, Watertown, MA) and consisted of denaturation at 95°C for 5 minutes; and 35 cycles: primer annealing at 96°C for 1 minute and extension at 68°C for 5 minutes. A separate genomic PCR assay to detect the wild-type allele (392-bp) or mutant *E2f1* allele (271-bp) was performed using the L31 intron primer (5′-GCTGGAATGGTGTCAGCACAGCG-3′) and the *E2f1* wild-type exon L26 primer (5′-TCCAAGAATCATATCCAGTGGCT-3′) or the neo^R gene primer. The E2F-1 was also genotyped using GGATATGATTCTTGGACTTCTTGG (E2F-1–5′) and CTAAATCTGACCACCAAACGC (E2F-1–3′) primers. PCR (25 μl) was performed using a PTC-200 for 39 cycles (94°C, 1 minute; 58°C, 1 minute; 72°C, 1 minute); and 1 cycle (72°C, 7 minutes); and then were analyzed using electrophoresis on a 2% agarose gel. A 100 base pair DNA ladder (TOYOBO Co., LTD, Osaka, Japan) was used as a marker.

Collection of Saliva and Determining Flow Volume. At 16–20 weeks old, NOD/LtJ, N11 (NOD/SCID.*E2f1*$^{-/-}$), N11 (NOD/SCID.*E2f1*$^{-/+}$), and N11 (NOD/SCID.*E2f1*$^{+/+}$) mice under anesthesia by intraperitoneal injection of 40~50 mg/kg sodium pentobarbital (Nembutal, Dainihon Pharmaceutical, Osaka, Japan) were injected with secretagogue, a mixture of isoproterenol (0.20 μg/100 g body weight) and pilocarpine (0.05 μg/100 g body weight; Sigma-Aldrich, St. Louis, MO) in PBS. Subsequently, saliva was collected for 15 minutes from the mouth into 1.5 ml microfuge tubes using a micropipette. The total volume was measured and calculated as per body weight; and the samples were then stored at –80°C for further analyses.

Histology Examination. Non-diabetic NOD, NOD/SCID.*E2f1*$^{-/-}$, NOD/SCID.*E2f1*$^{-/+}$, and NOD/SCID.*E2f1*$^{+/+}$ mice were sacrificed by CO_2 asphyxiation at 16–20 weeks of age after the blood serum was collected from orbital sinus under anesthesia by sodium pentobarbital. The mouse pancreas or submandibular salivary glands was cut into two equivalently sized sections where one of the sections was frozen and embedded in OCT compound (Sakura Finetechnical, Tokyo, Japan). The other section was immediately placed in 10% buffered formalin (Wako Chemical Co., Tokyo, Japan) for 96 hours prior to embedding in paraffin and sectioning. The sections from the formalin-fixed tissues were stained with hematoxylin and eosin for histology observation of mononuclear cell infiltration. Histology observations and photomicrography were performed using an Olympus BX50WI microscope (Olympus, Tokyo, Japan).

ELISA. For enzyme-linked immunosorbent assay (ELISA), 96-well microtiter H-plates (Sumitomo Bakelite, Tokyo, Japan) were coated overnight at 4°C with 1/500 goat anti-mouse immunoglobulin antibody (Cappel, West Chester, PA) in Na_2CO_3 coating buffer at pH 9.6. The plates were washed with PBS containing 0.1% (v/v) Tween 20 (PBST) and blocked with 1% (wt/vol) skim milk in PBST for 1 hour at 37°C. Excess skim milk was removed by washing three times with PBST then a 100 μl aliquot of a two-fold serial dilution of sera from the BC1 (NOD.*E2f1*$^{-/-}$ × NOD/SCID mice) was added to the wells; and the mixtures were incubated for 1 hour at 37°C. The wells were then washed five times with PBST; and further incubated for 1 hour at 37°C with 100 μl 1/1000 alkaline phosphatase-conjugated goat anti-mouse immunoglobulin M (both heavy and light chains) antibodies (Zymed Laboratories, South San Francisco, CA). After five washes with PBST, the bound antibodies were detected after the addition of 100 μl of 3 mg/ml *para*-nitrophenyl phosphate as a substrate and incubation for 30 minutes at 37°C. Absorbance at 405 nm (A_{405}) was measured using a microplate reader (Multiskan Bichromatic; Laboratory Japan, Tokyo, Japan). After 1 hour of incubation with the substrate, the ELISA antibody titer was expressed as the reciprocal (Log_2) of the highest dilution showing an A_{405} of 0.1 above the control (skim milk).

Immunohistochemistry. Immuno-staining was performed using a Vecta Stain Elite ABC Kit (Vector Laboratories, Burlingame, CA). The pancreases from the 4 month-old female non-diabetic NOD, NOD/SCID.*E2f1*$^{-/-}$, NOD/SCID.*E2f1*$^{-/+}$, and NOD/SCID.*E2f1*$^{+/+}$ mice were snap-frozen in OCT Compound and cut into 6 μm serial sections using a Cryostat (Microm, Zeiss, Germany) at –20°C. Endogenous peroxidase activity was inhibited using incubation with methanol containing 0.3% H_2O_2. The slides were washed in PBS; and the sections were incubated for 20 minutes with diluted normal blocking serum. Slides were then stained with 1/100 anti-mouse insulin (H-86) polyclonal antibodies (SC-9168, Santa Cruz Biotechnology, Santa Cruz, CA) or 1/100 anti-rabbit FGFR2 polyclonal antibody (Abgent, San Diego, CA) in a humidity chamber for 30 minutes at 37°C. Sections were rinsed in PBS; stained with biotinylated antibody solution for 30 minutes; and then sections were incubated in peroxidase substrate solution. 3–3-diaminobenzine tetrahydrochloridedehydrate (Vector Laboratories) was used as the chromogen. After washing in PBS, the sections were counterstained with methyl green stain solution (Muto Pure Chemicals Co., Tokyo, Japan), and then mounted with ENTELLANneu (Merck, Darmstadt, Germany).

α-Amylase Activity and Protein Concentration. Whole saliva samples were examined for amylase activity to hydrolyze starch using a Salivary α-Amylase Assay Kit (Salimetrics, State College, PA). Saliva samples were diluted with the α-amylase diluents to a final dilution of 1:200. Eight microliters of the diluted saliva samples were added to 320 μl preheated 37°C α-amylase substrate solution containing 2-chloro-p-nitrophenol and sodium azide at 0.01%; and mixed immediately by inversion. Absorbance was measured at 405 nm. The protein concentration in the saliva samples was measured using a Bio-Rad Protein Assay (Bio-Rad Laboratories, Hercules, CA) based on the method of Bradford, an accurate procedure for determining the concentration of solubilized protein that involves the addition of an acidic dye to the protein solution and subsequent measurement at 595 nm.

Statistical Analysis. The Kaplan-Meier cumulative survival estimate and the log-rank test were used to compare the incidence of diabetes and death. Comparative analyses were performed using the one-way analysis of variance (ANOVA) followed by Tukey's honestly significant difference (HSD) *post hoc* test. A $P < 0.05$ was considered to be statistically significant for two-tailed comparisons. All statistical analyses were performed using the SPSS II ver.11.0.1J (SPSS Inc., Chicago, IL).

Results

Replacement of the SCID Gene in NOD.*E2f1*$^{-/-}$ Mice. To produce F1 (NOD.*E2f1*$^{-/-}$ × NOD/SCID) mice, NOD.*E2f1*$^{-/-}$ mice were first mated with NOD/SCID mice. Development of diabetes was observed in the F1 females at

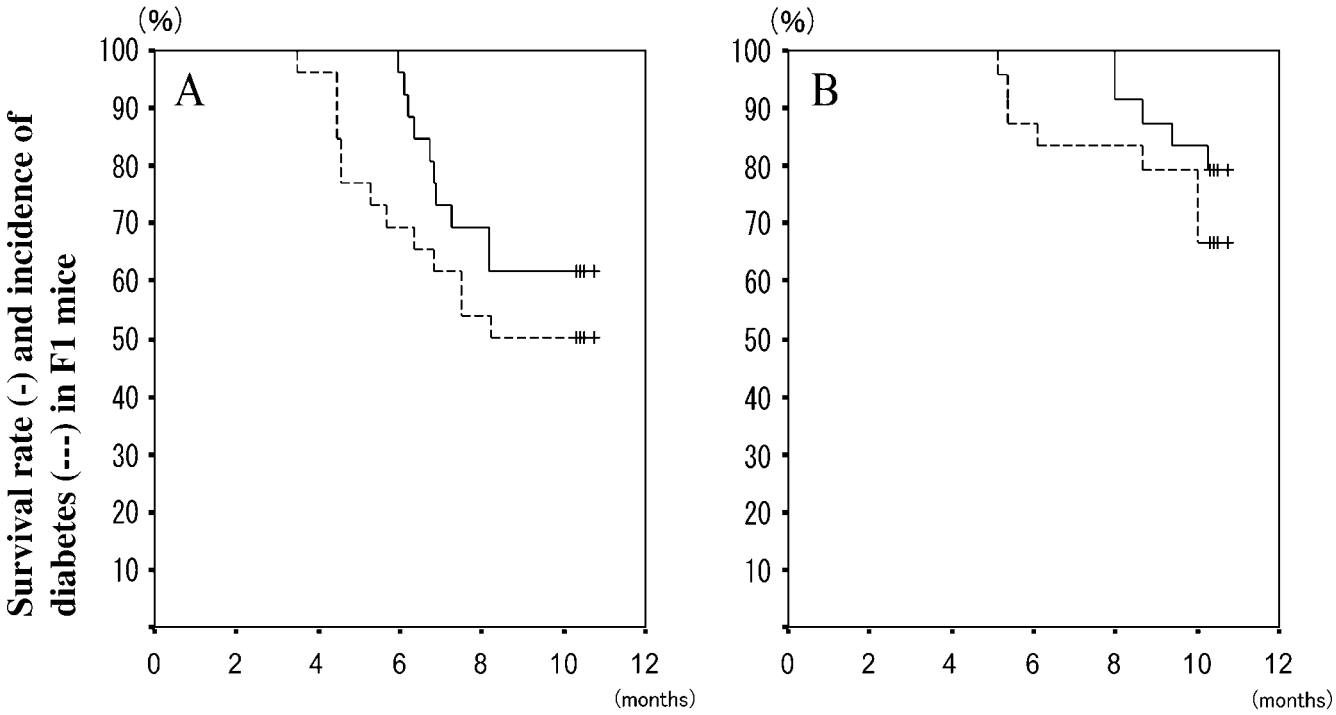

Figure 1. Survival of F1 (NOD.*E2f1*$^{-/-}$ × NOD/SCID) mice. The survival (-) and development of diabetes (- - -) of F1 [NOD/SCID x NOD.*E2f-1*$^{-/-}$; 26 female (A) and 24 male (B)] were scored. The vertical short lines indicate month age limit survival and development of diabetes.

more than 3 months of age and in the F1 males at more than 5 months (Fig. 1). All of the diabetic mice died within 2 months of development of diabetes. As a next strain, BC1 mice were produced by backcrossing the F1 mice and the NOD/SCID mice. BC1 mice were screened by PCR analysis for the product of the neo^{R} gene and using ELISA for IgM production in serum. Typical data for BC1 mice are shown in Figure 2. BC1 001 and BC4 004 did not produce IgM (Fig. 2A) and did not possess the neo^{R} gene (Fig. 2B), and, therefore, were characterized as NOD/SCID$^{+/+}$.*E2f1*$^{+/+}$. BC1 002 did not produce IgM (Fig. 2A) but possessed the neo^{R} gene (Fig. 2B), and were characterized as NOD/SCID$^{+/+}$.*E2f1*$^{-/+}$. BC1 003 produced IgM (Fig. 2A) but did not possess the neo^{R} gene (Fig. 2B), and were characterized as NOD/SCID$^{-/+}$.*E2f1*$^{+/+}$. BC1 005 produced IgM (Fig. 2A) and possessed the neo^{R} gene (Fig. 2B), and were characterized as NOD/SCID$^{-/+}$.*E2f1*$^{-/+}$. All BC1 mice were finally divided into four mice groups: NOD/SCID$^{-/+}$.*E2f1*$^{-/+}$, NOD/SCID$^{-/+}$.*E2f1*$^{+/+}$, NOD/SCID$^{+/+}$.*E2f1*$^{-/+}$, and NOD/SCID$^{+/+}$.*E2f1*$^{+/+}$. The NOD/SCID$^{+/+}$.*E2f1*$^{+/+}$ female and male mice did not develop diabetes; however, dead mice were observed at more than 80% of the population at the age

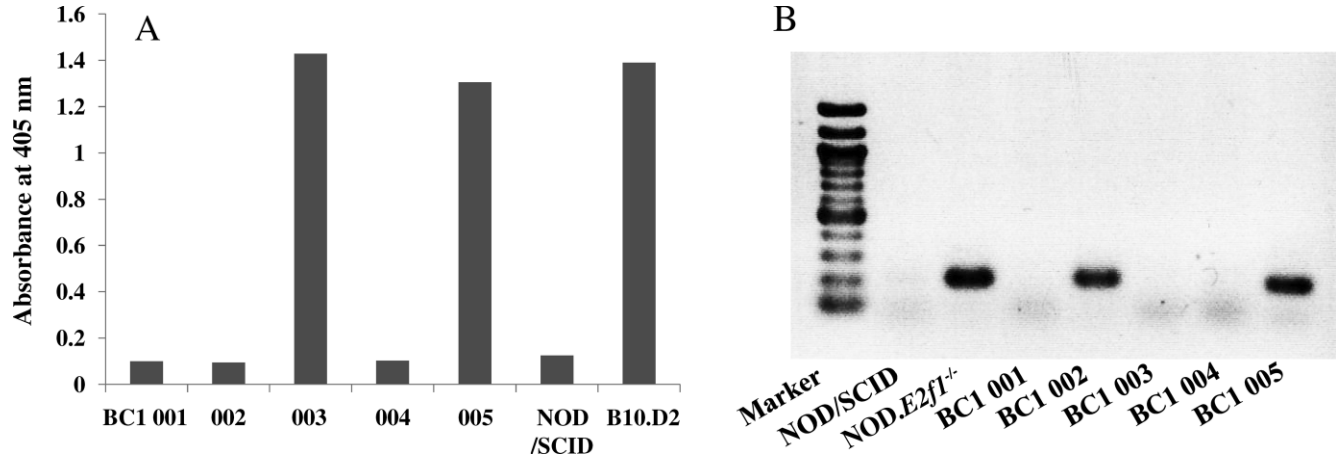

Figure 2. Screening for IgM production and neo^{R} presence in BC1 (F1 × NOD/SCID). Serum IgM from some (BC1 001~005) BC1 (F1 × NOD/SCID) was measured using ELISA (A). Presences of neo^{R} from some BC1 mice were tested using PCR (B). Typical results are presented. NOD/SCID and B10.D2 mice were used as a negative and positive control, respectively, in the ELISA. NOD/SCID and NOD.*E2f1*$^{-/-}$ were used as a negative and positive, respectively, for controls in PCR analysis. Marker: 100 bp DNA ladder.

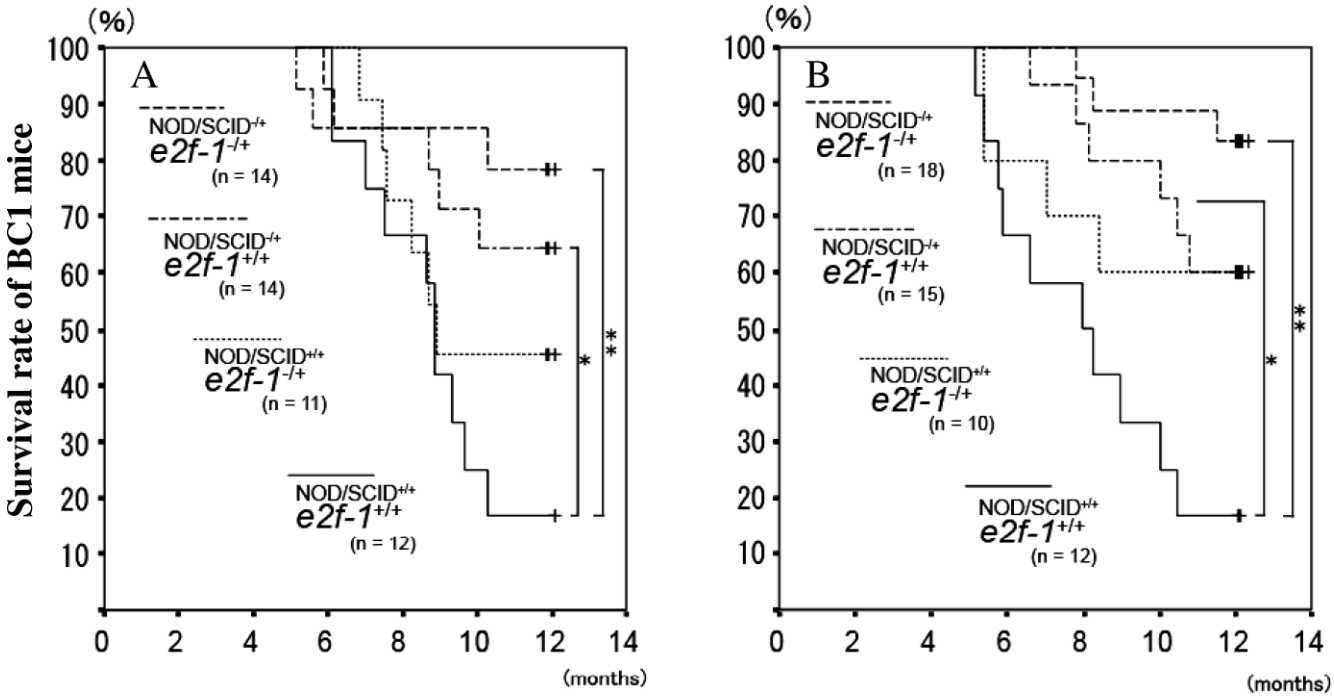

Figure 3. Survival curves of BC1 (F1 × NOD/SCID). BC1 mice were produced by backcrossing of F1 and NOD/SCID mice. The survival of BC1 [the respective numbers of female (A) and male (B) mice were: NOD/SCID$^{-/+}$.*E2f1*$^{-/+}$: $n = 14$ and 18, NOD/SCID$^{-/+}$.*E2f1*$^{+/+}$: $n = 14$ and 15, NOD/SCID$^{+/+}$.*E2f1*$^{-/+}$: $n = 11$ and 10, and NOD/SCID$^{+/+}$.*E2f1*$^{+/+}$: $n = 12$ and 12, respectively] were scored. Vertical short lines indicate the month age limit of survival and development of diabetes. Asterisks show significantly different relative levels of survival (* $P < 0.05$, NOD/SCID$^{+/+}$.*E2f1*$^{+/+}$ vs. NOD/SCID$^{-/+}$.*E2f1*$^{+/+}$, ** $P < 0.01$, NOD/SCID$^{+/+}$.*E2f1*$^{+/+}$ vs. NOD/SCID$^{-/+}$.*E2f1*$^{-/+}$).

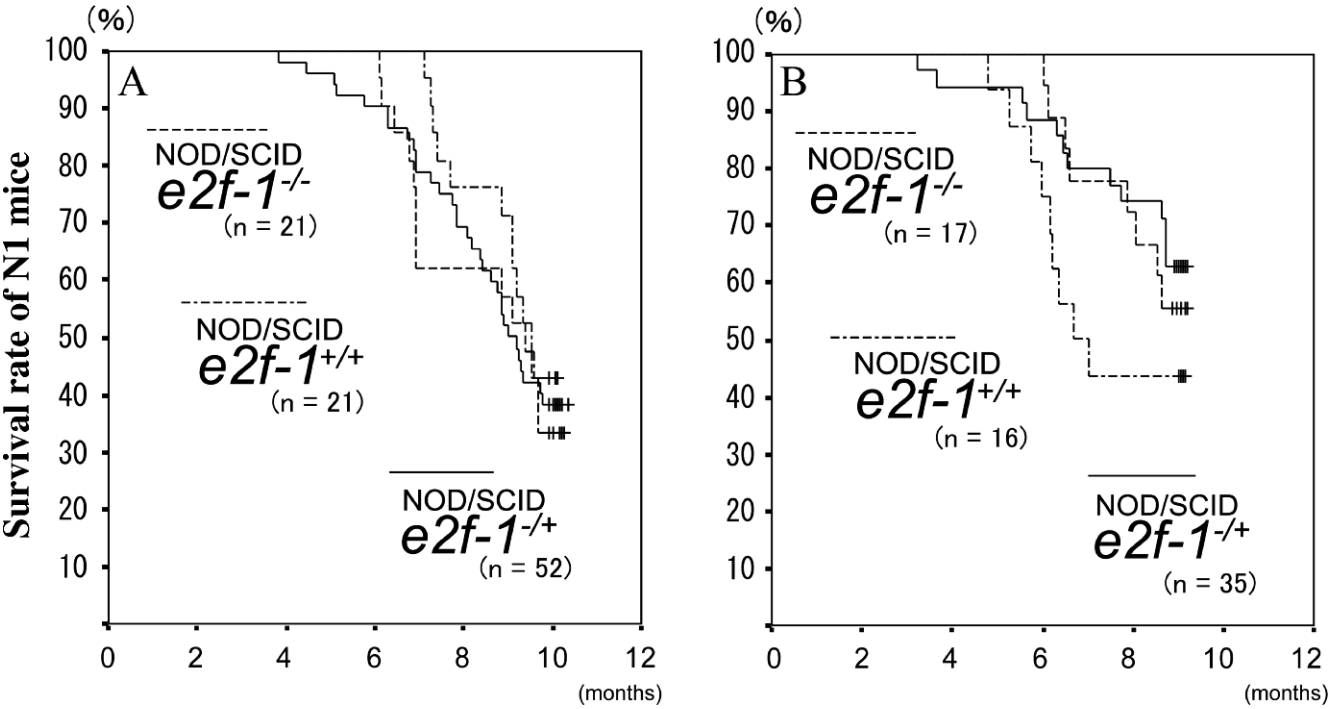

Figure 4. Survival curves of intercross mice (NOD/SCID.*E2f1*$^{-/-}$ × NOD/SCID.*E2f1*$^{-/-}$). The intercross mice were divided into NOD/SCID.*E2f1*$^{+/+}$ (21 female and 16 male), NOD/SCID.*E2f1*$^{-/+}$ (52 female and 35 male), and NOD/SCID.*E2f1*$^{-/-}$ (21 female and 17 male). The survival of the intercross mice for female (A) and male (B) were scored. Vertical short lines indicate the month age limit of survival and development of diabetes.

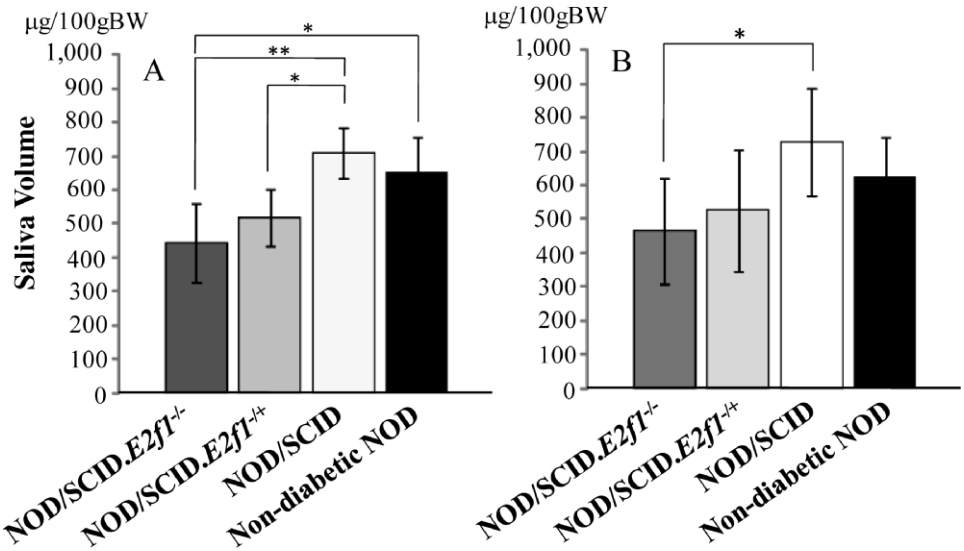

Figure 5. Salivary volumes for NOD, NOD/SCID, NOD/SCID.*E2f1*$^{-/+}$, and NOD/SCID.*E2f1*$^{-/-}$ mice [female (A) and male (B)]. Total volume of secreted saliva per 100 g of body weight for each mouse was measured. Data are expressed as the means ± SD of 5~7 mice. Asterisks show significant differences (* $P < 0.05$: NOD/SCID vs. NOD/SCID.*E2f1*$^{-/-}$ in males, NOD/SCID vs. NOD/SCID.*E2f1*$^{-/+}$, and NOD vs. NOD/SCID.*E2f1*$^{-/-}$ in females; ** $P < 0.01$: NOD/SCID vs. NOD/SCID.*E2f1*$^{-/-}$ in females).

of 12 months (Fig. 3A and B). Development of diabetes was observed in three of 14 NOD/SCID$^{-/+}$.*E2f1*$^{-/+}$ and five of 14 NOD/SCID$^{-/+}$.*E2f1*$^{+/+}$ female mice; and in three of 18 NOD/SCID$^{-/+}$.*E2f1*$^{-/+}$ and three of 15 NOD/SCID$^{-/+}$.*E2f1*$^{+/+}$ male mice. However, the survival rate at 12 months was significantly higher among the NOD/SCID$^{-/+}$.*E2f1*$^{-/+}$ mice and NOD/SCID$^{-/+}$.*E2f1*$^{+/+}$ mice compared to the NOD/SCID$^{+/+}$.*E2f1*$^{+/+}$ mice (Fig. 3). The intercross mice were produced by intercrossing NOD/SCID$^{+/+}$.*E2f1*$^{-/+}$ mice divided into three groups: NOD/SCID$^{+/+}$.*E2f1*$^{+/+}$, NOD/SCID$^{+/+}$.*E2f1*$^{-/+}$, and NOD/SCID$^{+/+}$.*E2f1*$^{-/-}$ mice; screened for development of diabetes and insulitis, and the number of dead mice at 12 months. No E2*f*1 expression was found using PCR analysis in the NOD/SCID$^{+/+}$.*E2f1*$^{-/-}$ mice. However, there were no significant differences in the survival rate of females and males among the groups (Fig. 4A and B). They did not develop diabetes and insulitis at 12 months. Further, the immunohistochemistry analyses using anti-insulin antibody, performed to define production of insulin in β cells of the Langerhans islets, showed no clear differences among the three groups (data not shown).

To study the role of E2F-1 in the function of the salivary gland, the volume of secreted saliva at 15 minutes after stimulation using isoproterenol and pilocarpine was measured. The secretion of saliva decreased at many time points after the stimulation in NOD/SCID.*E2f1*$^{-/-}$ females and males in comparison to NOD/SCID.*E2f1*$^{+/+}$ mice (data not shown). The secretion total volume was significantly lower in females of NOD/SCID.*E2f1*$^{-/-}$ compared to NOD/SCID and NOD non-diabetic mice at 15 minutes after the stimulation (Fig. 5A). The secretion total volume was significantly lower in NOD/SCID.*E2f1*$^{-/+}$ compared to NOD/SCID mice (Fig. 5A). In male mice, the secretion volume was significantly lower in NOD/SCID.*E2f1*$^{-/-}$ compared to NOD/SCID mice (Fig. 5B). We characterized the saliva from three mice from each group where the protein concentration and amylase activities were measured; however, there were no significant differences in the three groups and in the NOD mice (Fig. 6A, B, C, and D). After recalculation using the protein concentration and saliva production volume, the production of protein per minute in 1 ml of saliva was significantly lower in NOD/SCID.*E2f1*$^{-/-}$ females as compared to NOD/SCID mice (Fig. 6E). In the males, however, there were no significant differences among the three groups and the NOD mice (Fig. 6F).

To determine the mechanism for decreased saliva volume in the NOD/SCID.*E2f1*$^{-/-}$ mice, histological analysis was performed on all intercross mice. Infiltration of lymphocytes was observed in the salivary glands from NOD mice but not in any of the intercross mice (Fig. 7). Interestingly, the nuclear size was larger in the salivary gland cells from NOD/SCID.*E2f1*$^{-/-}$ mice compared to NOD/SCID and NOD mice (arrow, Fig. 8). Further, the increase in the number of ducts was higher in the NOD/SCID.*E2f1*$^{-/-}$ and NOD.*E2f1*$^{-/-}$ compared to the NOD/SCID and NOD mice (Fig. 7). Expression of FGFR-2b is associated with the development of the submandibular gland (29–31) and E2F-1 activity. Therefore, the protein localization was measured using immunohistochemistry with anti-FGFR-2b polyclonal antibody in NOD, NOD/SCID, NOD/SCID.*E2f1*$^{-/+}$, and NOD/SCID.*E2f1*$^{-/-}$ mice. The protein localization of FGFR-2b was strongly observed in NOD and NOD/SCID mice; weakly in NOD/SCID.*E2f1*$^{-/+}$ mice; and poorly around tissues of some ducts in NOD/SCID.*E2f1*$^{-/-}$ mice (Fig. 9).

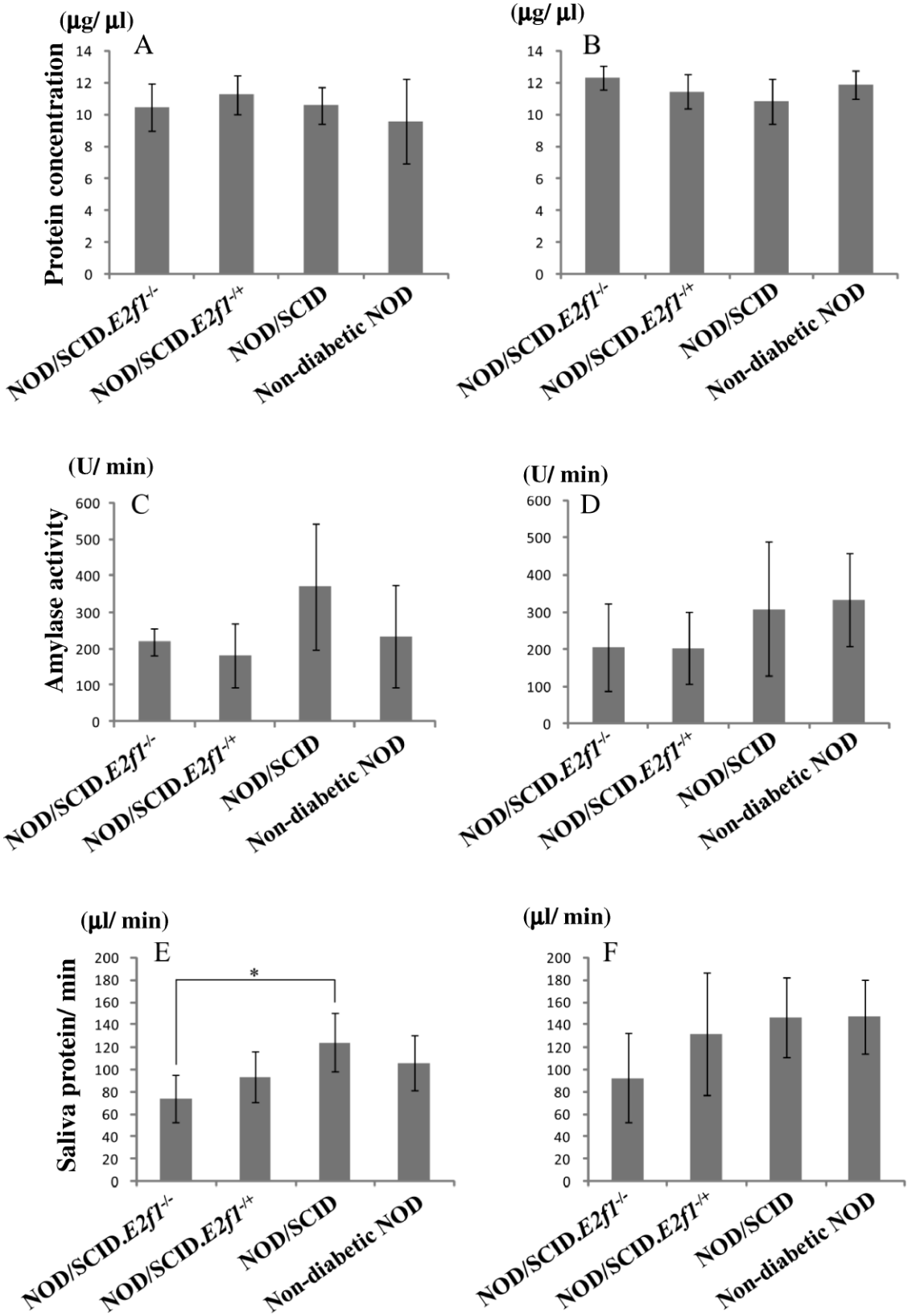

Figure 6. Comparison of the biochemical change in saliva between NOD, NOD/SCID, NOD/SCID.*E2f1*$^{-/+}$, and NOD/SCID.*E2f1*$^{-/-}$ mice [females: (A), (C), and (E); males: (B), (D), and (F)]. Protein concentration (A and B), amylase activity (C and D) and saliva protein/min (E and F) were measured. Data are expressed as the means ± SD for 5~7 mice per strain (* $P < 0.05$).

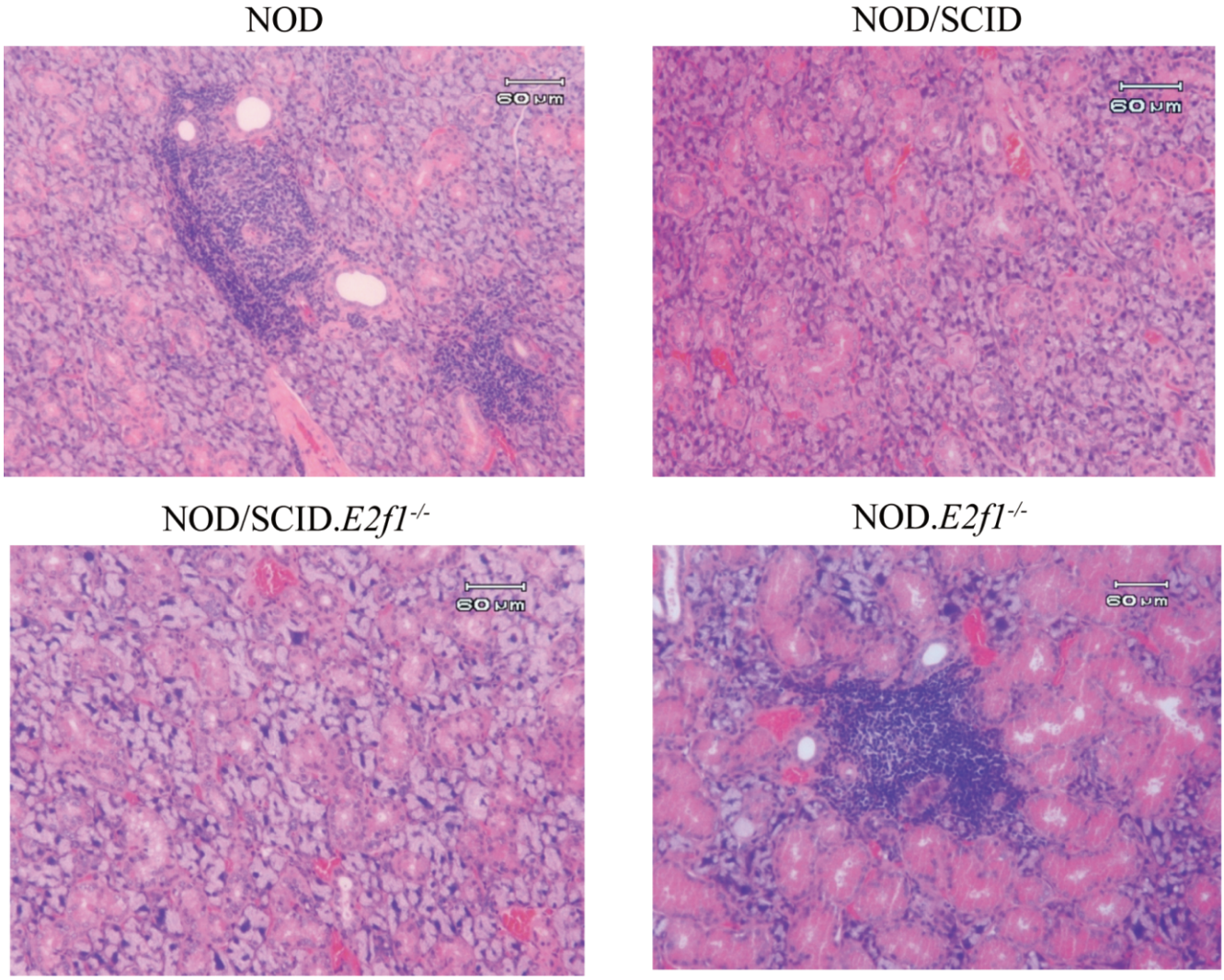

Figure 7. Photomicrographs of submandibular glands at 4 months of age in NOD, NOD/SCID, NOD/SCID.*E2f1*$^{-/-}$, and NOD.*E2f1*$^{-/-}$ mice (H-E ×200). The typical histology in a NOD and NOD/SCID mouse where the ducts are normally shown in the salivary gland is a control. Higher numbers of ducts from NOD/SCID.*E2f1*$^{-/-}$ were found compared to NOD and NOD/SCID mice. A color version of this figure is available in the online journal.

Discussion

In our previous report (27), NOD.*E2f1*$^{-/-}$ mice showed a more progressive development of diabetes and Sjögren syndrome than did NOD mice. We found a decrease in regulatory T cells ($CD4^+CD25^+$) and expression of auto-reactive Th1-type T cells, and the possibility of a progressive reduction in the systemic secretion systems of insulin and saliva. Therefore, we concluded that further study of the mechanism of early-onset diabetes in E2F-1-deficient NOD mice was required by producing E2F-1-deficient NOD/SCID mice in which T and B cells do not develop. Here we generated E2F-1-deficient NOD/SCID mice, and surveyed for the development of diabetes, insulitis, and production of saliva. The inhibition in maturation of T cells and B cells in NOD.*E2f1*$^{-/-}$ mice prevented naturally both diabetes and insulitis and the infiltration of lymphocytes into salivary glands; and did not prevent a decrease in the production of saliva. The production of insulin in β cells from the islets in the wild-type was not different compared to the E2F-1-deficient NOD/SCID mice. Therefore, we determined the combination of the E2F-1 deficiency in the NOD background induces a decrease in the regulatory T cells and an increase in auto-reactive T cells as shown in the previous study (27); and neither combination was associated with T and B cells-independent dysfunction in the pancreatic β cells for insulin secretion in this study. Moreover, the association of E2F-1 with T and B cells-independent dysfunction of the salivary gland in the NOD background was another finding in this study. E2F-1 induces spontaneous apoptosis. It was previously postulated that tissue-specific E2F-1 dependent apoptosis in exocrine glands may contribute to Sjögren's syndrome (32). Therefore, the regulation of E2F-1 may be central to the production of saliva. In this study, the effects

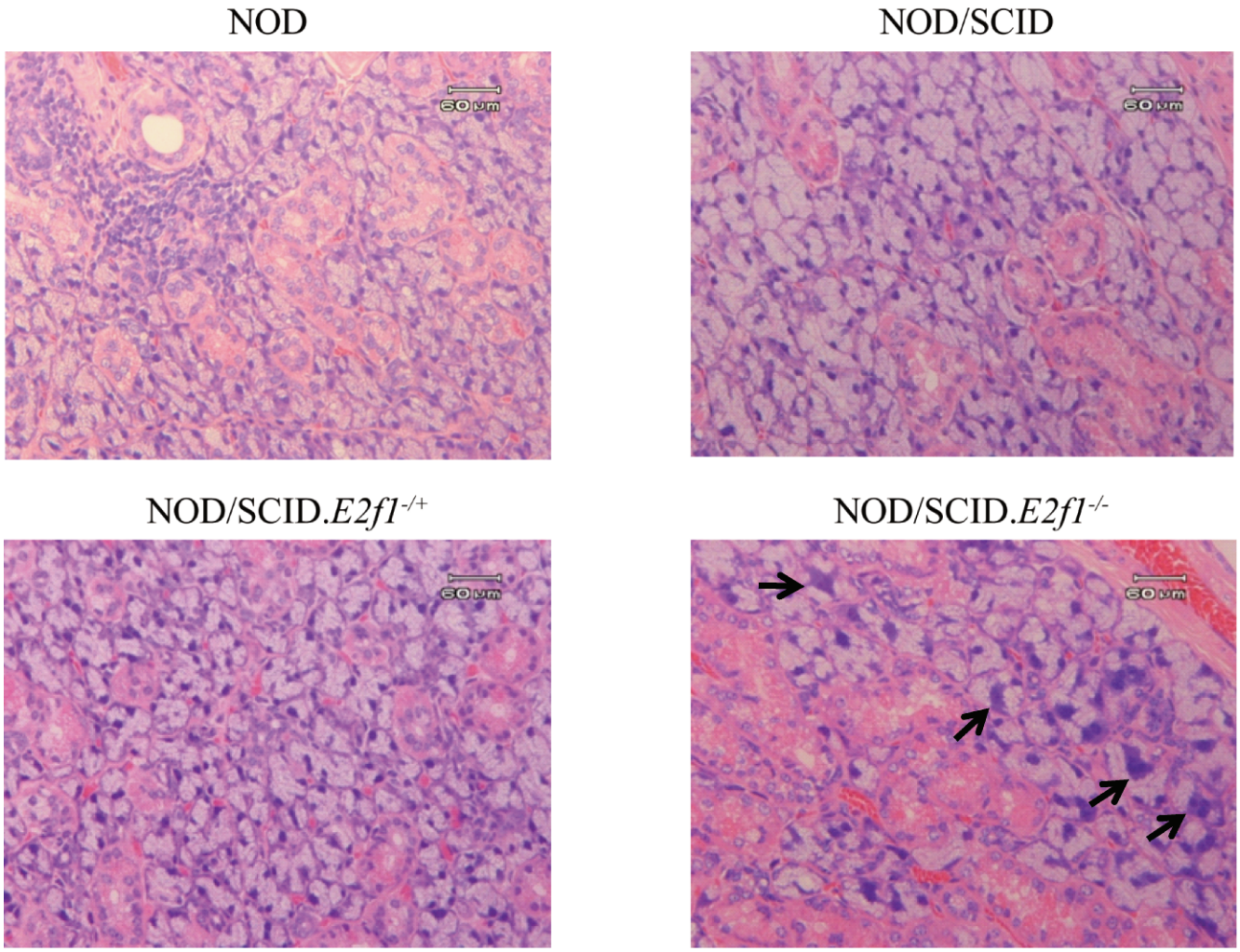

Figure 8. Photomicrographs of submandibular glands at 4 months of age in NOD, NOD/SCID, NOD/SCID.*E2f1*$^{-/+}$ and NOD/SCID.*E2f1*$^{-/-}$ mice (H-E ×400). A typical histology for the NOD and NOD/SCID mouse where the normal nuclear size is shown in the salivary gland as a control. The nuclear size of NOD/SCID.*E2f1*$^{-/-}$ mice was larger compared to the NOD and NOD/SCID mouse. A color version of this figure is available in the online journal.

of the E2F-1 deficiency were clearly observed in the NOD/SCID background where a higher production volume of saliva was expected compared to the B6 background (33, 34). The percent inhibition of saliva production volume (μl/100 g BW) in NOD non-diabetic mice having the E2F-1 deficiency was slightly higher in NOD female mice (38.1%) (27) than in NOD/SCID female mice (33.1%) (Fig. 5). Therefore, we consider the contribution to develop auto-reactive T cells in the progression of saliva decrease was poor in NOD.*E2f1*$^{-/-}$ mice. The systemic dysfunction of the salivary gland by E2F-1 deficiency is the principal reason for the decrease in saliva in the mice.

Fibroblast growth factor (FGF) is thought to regulate cellular proliferation, differentiation, and migration; and also acts as a major ligand for the FGF receptor 2IIIb (FGFR-2b) in mouse multi-organ development (29). Further, FGF and FGFR-2b proteins play an important role in angiogenesis and embryonic development. The expression of FGFR-2 is induced in the mid-to-late G1 phase of the cell cycle. Transcription of mouse FGFR-2 was activated by E2F-1 (35) that controls the G1 phase of the cell cycle. In the above reports, it is suggested the signaling of FGFR-2b with FGF-10 is associated with E2F-1 activity. Interestingly, the interaction between FGF-10, one of the FGF family, and FGFR-2b are required for the development of the mouse's submandibular glands (28–30). Further, FGF-10 heterozygous mice are viable and fertile but display hypoplasia of the submandibular and the lacrimal gland (36, 37). FGFR-2b signaling regulates submandibular gland proliferation and morphogenesis (38). We believe, based on both of the works cited above and here, that the saliva in the strains of mice we developed had less volume because the salivary glands do not develop because there is no signal of FGFR-2 to FGF-10. Another phenotype in this study that shows increasing numbers of ducts in the submandibular glands was observed in E2F-1-deficient NOD/SCID mice in comparison to the wild-type NOD/SCID mice. FGF-10 is highly expressed in the condensing submandibular gland

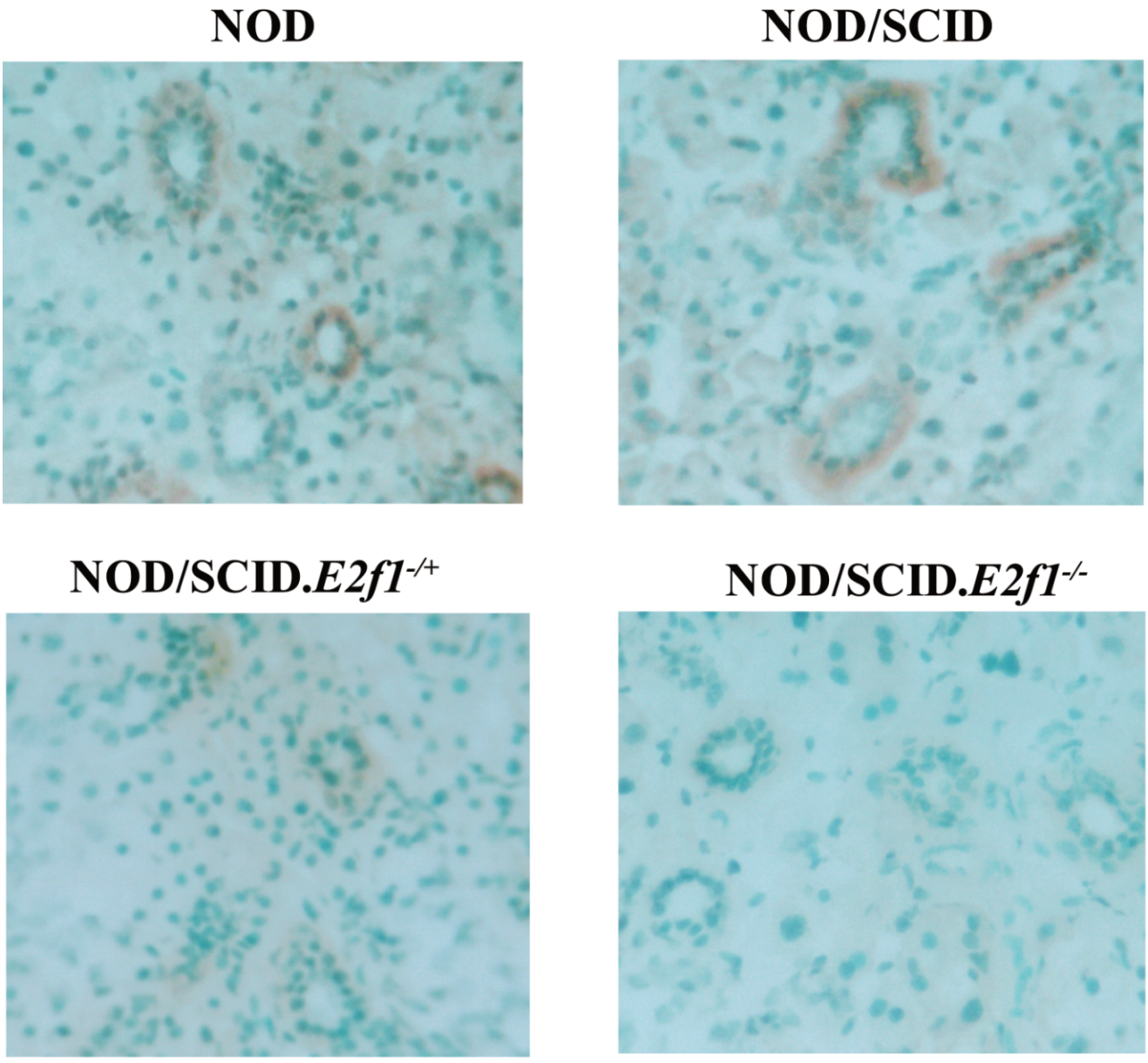

Figure 9. Immunohistochemical protein localization of FGFR-2 in salivary glands from NOD, NOD/SCID, NOD/SCID.*E2f1*$^{-/+}$ and NOD/SCID.*E2f1*$^{-/-}$ mice. Photomicrographs of submandibular glands reacting with anti-FGFR-2 antibody are shown. A typical immunohistology appearance in a NOD mouse where the ducts express FGFR-2 (red color) is shown as a positive control. The expression of FGFR-2 was poorly observed in NOD/SCID.*E2f1*$^{-/-}$ mice.

mesenchyma; whereas FGFR-2b is found in the initial epithelial bud that forms on the end of a single primary duct (39). In a recent report, heparan sulfate modulates specific FGF-10-mediated events such as proliferation, duct elongation, end bud expansion, and differentiation (40). The protein localization of FGFR-2b disappeared in NOD/SCID.*E2f1*$^{-/-}$ as compared to the NOD/SCID wild-type mice. The reasons for the phenotype in E2F-1 and FGFR-2b were clearly demonstrated here and in previous reports where the immature development of ducts may be associated with the increased number of ducts, decreasing volume of saliva and expression of FGFR-2b in the ducts of the salivary glands. A definitive analysis of the mechanism regarding the relationship between FGF-10 and FGFR-2b in the differentiation of duct and acinar cells in salivary glands from E2F-1-deficient NOD/SCID mice requires further molecular and genetic investigations.

The pancreas contains two distinct populations of cells referred to as endocrine and exocrine cells. The insulin-producing β cells are endocrine cells in the pancreas islets. FGF-10 functions as a stimulator of pancreatic exocrine development (41, 42). The pancreatic progenitor cells present in the early pancreatic analogen can proliferate and generate the full complement of pancreatic epithelial cell types. FGFR-2b is linked to pancreatic epithelial cell proliferation (43, 44). FGF-10 signaling mediated by the

FGFR-2b receptor is required for the expansion and differentiation of exocrine cells in the embryonic pancreas (45). Therefore, we conclude that the inactivation of FGFR-2b occurs through an E2F-1 deficiency that affects differentiation of the exocrine cells in the salivary glands; but does not affect the differentiation of the endocrine cells from the β cells of the pancreas islets.

F1 (NOD.*E2f1*$^{-/-}$ × NOD/SCID) mice developed diabetes because auto-reactive T cells with IgM and IgG antibodies were also induced in SCID-heterologous NOD.*E2f1*$^{-/-}$ mice. Two type strains of BC1 (F1 × NOD/SCID, NOD/SCID$^{-/+}$.*E2f1*$^{+/+}$, and NOD/SCID$^{-/+}$.*E2f1*$^{-/+}$) mice developed diabetes slightly but other strains, NOD/SCID$^{+/+}$.*E2f1*$^{+/+}$ and NOD/SCID$^{+/+}$.*E2f1*$^{-/+}$, did not. In contrast, the rate of death was significantly higher among NOD/SCID$^{+/+}$.*E2f1*$^{+/+}$ mice than among NOD/SCID$^{-/+}$.*E2f1*$^{+/+}$ or NOD/SCID$^{-/+}$.*E2f1*$^{-/+}$ mice. Life is shorter among the homozygous SCID mice than among heterozygous SCID mice that develop diabetes in the NOD genetic background. But the heterozygous recombination of the E2F-1-deficient gene did not influence death in mice. The intercross mice [BC1 (NOD/SCID$^{+/+}$*E2f1*$^{-/+}$) × BC1 (NOD/SCID$^{+/+}$.*E2f1*$^{-/+}$)] did not develop diabetes but death appeared at an age of more than 3 months. However, there was no significant difference in survival rate among the intercross mice groups; and therefore, the E2F-1 deficiency did not affect the survival rate. The NOD/SCID$^{+/+}$.*E2f1*$^{-/-}$ did not develop diabetes or decreased production of saliva, and are a stable source for *in vivo* experiments where this strain may be useful as a high-susceptibility model for oral infections.

SCID and NOD/SCID mice are used for humanized mouse experiments for engraftment of human tissues and cells (46–49). Recently, NOG mice and SCID.IFN-γ$^{-/-}$ were also established as high recipients for engraftments (50, 51). Many investigators are studying new types of humanized mice. The NOD/SCID.*E2f1*$^{-/-}$ mouse is a new type of humanized mouse that may be useful as a saliva-decreased humanized mouse for oral infections by bacteria and viruses.

In conclusion, we created E2F-1-deficient NOD/SCID mice showing a decreased volume of saliva; but not diabetes insulitis or infiltration of lymphocytes into the salivary glands. E2F-1 may be associated with the differentiation of exocrine cells from duct cells where FGFR-2b is localized in salivary glands. E2F-1 controls the regulatory T cells and auto-reactive T cells in the development of diabetes in NOD mice. E2F-1- deficient NOD/SCID mice may be useful for various experiments on humanized mice and oral infections.

The authors thank Naoki Narisawa, Taisuke Fujibayashi, Moriyuki Nakamura, Abdus Salam, and Ryoma Nakao for their technical support, helpful discussions, and advice.

1. Salomon B, Lenschow DJ, Rhee L, Ashourian N, Singh B, Sharpe A, Bluestone JA. B7/CD28 costimulation is essential for the homeostasis of the CD4^{+}CD25^{+} immunoregulatory T cells that control autoimmune diabetes. Immunity 12:431–440, 2000.
2. Hattori M, Yamato E, Itoh N, Senpuku H, Fujisawa T, Yoshino M, Fukuda M, Matsumoto E, Toyonaga T, Nakagawa I, Petruzzelli M, McMurray A, Weiner H, Sagai T, Moriwaki K, Shiroishi T, Maron R, Lund T. Cutting edge: homologous recombination of the MHC class IK region defines new MHC-linked diabetogenic susceptibility gene(s) in nonobese diabetic mice. J Immunol 163:1721–1724, 1999.
3. Anderson MS, Bluestone JA. The NOD mouse: a model of immune dysregulation. Annu Rev Immunol 23:447–485, 2005.
4. Daniels TE, Fox PC. Salivary and oral components of Sjögrens-syndrome. Rheum Dis Clin North Am 18:571–589, 1992.
5. Wicker LS, Appel MC, Dotta F, *et al*. Autoimmune syndromes in major histocompatibility complex (MHC) congenic strains of nonobese diabetic (NOD) mice—the NOD MHC is dominant for insulitis and cyclophosphamide-induced diabetes. J Exp Med 176:67–77, 1992.
6. Wicker LS, Miller BJ, Coker LZ, McNally SE, Scott S, Mullen Y, Appel MC. Genetic control of diabetes and insulitis in the nonobese diabetic (NOD) mouse. J Exp Med 165:1639–1654, 1987.
7. Makino S, Kunimoto K, Muraoka Y, Mizushima Y, Katagiri K, Tochino Y. Breeding of a non-obese, diabetic strain of mice. Jikken Dobutsu 29:1–13, 1980.
8. Jansen A, Homo-Delarche F, Hooijkaas H, Leenen PJ, Dardenne M, Drexhage HA. Immunohistochemical characterization of monocytes-macrophages and dendritic cells involved in the initiation of the insulitis and beta-cell destruction in NOD mice. Diabetes 43:667–675, 1994.
9. Jonsson R, Kroneld U, Backman K, Magnusson B, Tarkowski A. Progression of left out rest sialadenitis in Sjögrens-syndrome. Br J Rheumatol 32:578–581, 1993.
10. Humphreys-Beher MG, Brayer J, Yamachika S, Peck AB, Jonsson R. An alternative perspective to the immune response in autoimmune exocrinopathy: induction of functional quiescence rather than destructive autoaggression. Scand J Immunol 49:7–10, 1999.
11. Bolstad AI, Jonsson R. Genetic aspects of Sjögren's syndrome. Arthritis Res 24:353–359, 2002.
12. Robinson CP, Yamachika S, Bounous DI, Brayer J, Jonsson R, Holmdahl R, Peck AB, Humphreys-Beher MG. A novel NOD-derived murine model of primary Sjögren's syndrome. Arthritis Rheum 41: 150–156, 1998.
13. Salam MA, Matin K, Matsumoto N, Tsuha Y, Hanada N, Senpuku H. Establishment of an animal model using recombinant NOD.B10.D2 mice to study initial adhesion of oral streptococci. Clin Diagn Lab Immunol 11:379–386, 2004.
14. Tsantoulis PK, Gorgoulis VG. Involvement of E2F transcription factor family in cancer. Eur J Cancer 41:2403–2414, 2005.
15. Cam H, Dynlacht BD. Emerging roles for E2F: beyond the G1/S transition and DNA replication. Cancer Cell 3:311–316, 2003.
16. DeGregori J. The genetics of the E2F family of transcription factors: shared functions and unique roles. Biochim Biophys Acta 1602:131–150, 2002.
17. Serrano M, Lin AW, McCurrach ME, Beach D, Lowe SW. Oncogenic ras provokes premature cell senescence associated with accumulation of p53 and p16INK4a. Cell 88:593–602, 1997.
18. Bell LA, Ryan KM. Life and death decisions by E2F-1. Cell Death Differ 11:137–142, 2004.
19. Wyllie AH. E2F1 selects tumour cells for both life and death. J Pathol 198:139–141, 2002.
20. Ginsberg D. E2F1 pathways to apoptosis. FEBS Lett 529:122–125, 2002.
21. Murga M, Fernandez-Capetillo O, Field SJ, Moreno B, Borlado LR, Fujiwara Y, Balomenos D, Vicario A, Carrera AC, Orkin SH, Greenberg ME, Zubiaga AM. Mutation of E2F2 in mice causes enhanced T lymphocyte proliferation, leading to the development of autoimmunity. Immunity 15:959–970, 2001.

22. Field SJ, Tsai FY, Kuo F, Zubiaga AM, Kaelin WG Jr, Livingston DM, Orkin SH, Greenberg ME. E2F-1 functions in mice to promote apoptosis and suppress proliferation. Cell 85:549–561, 1996.
23. Yamasaki L, Jacks T, Bronson R, Goillot E, Harlow E, Dyson NJ. Tumor induction and tissue atrophy in mice lacking E2F-1. Cell 85: 537–548, 1996.
24. Zhu JW, DeRyckere D, Li FX, Wan YY, DeGregori J. A role for E2F1 in the induction of ARF, p53, and apoptosis during thymic negative selection. Cell Growth Differ 10:829–838, 1999.
25. Rounbehler RJ, Rogers PM, Conti CJ, Johnson DG. Inactivation of E2f1 enhances tumorigenesis in a Myc transgenic model. Cancer Res 62:3276–3281, 2002.
26. Lillibridge CD, O'Connell BC. In human salivary gland cells, overexpression of E2F1 overcomes an interferon-gamma- and tumor necrosis factor-alpha-induced growth arrest but does not result in complete mitosis. J Cell Physiol 172:343–350, 1997.
27. Salam MA, Matin K, Matsumoto N, Tsuha Y, Hanada N, Senpuku H. E2f1 mutation induces early onset of diabetes and Sjögren's syndrome in nonobese diabetic mice. J Immunol 173:4908–4918, 2004.
28. Iglesias A, Murge M, Laresgoiti U, Skoudy A, Bernales I, Fullaondo A, Moreno B, Lloreta J, Field SJ, Real FX, Zubiaga AM. Diabetes and exocrine pancreatic insufficiency in E2F1/E2F2 double-mutant mice. J Clin Invest 113:1398–1407, 2004.
29. Ohuchi H, Hori Y, Yamasaki M, Harada H, Sekine K, Kato S, Itoh N. FGF10 acts as a major ligand for FGF receptor 2 IIIb in mouse multi-organ development. Biochem Biophys Res Commun 277:643–649, 2000.
30. Min H, Danilenko DM, Scully SA, Bolon B, Ring BD, Tarpley JE, DeRose M, Simonet WS. Fgf-10 is required for both limb and lung development and exhibits striking functional similarity to Drosophila branchless. Genes Dev 12:3156–3161, 1998.
31. Sekine K, Ohuchi H, Fujiwara M, Yamasaki M, Yoshizawa T, Sato T, Yagishita N, Matsui D, Koga Y, Itoh N, Kato S. Fgf10 is essential for limb and lung formation. Nat Genet 21:138–141, 1999.
32. Ishimaru N, Arakaki R, Omotehara F, Yamada K, Mishima K, Saito I, Hayashi Y. Novel role for RbAp48 in tissue-specific, estrogen deficiency-dependent apoptosis in the exocrine glands. Mol Cell Biol 26:2924–2935, 2006.
33. Matsumoto N, Salam MA, Watanabe H, Amagasa T, Senpuku H. Role of gene E2F1 in susceptibility to bacterial adherence of oral streptococci to tooth surfaces in mice. Oral Microbiol Immunol 19: 270–276, 2004.
34. Matin K, Salam MA, Akhter J, Hanada N, Senpuku H. Role of stromal-cell derived factor-1 in the development of auto immune diseases in non-obese diabetic mice. Immunology 107:222–231, 2002.
35. Tashiro E, Minato Y, Maruki H, Asagiri M, Imoto M. Regulation of FGF receptor-2 expression by transcription factor E2F-1. Oncogene 22: 5630–5635, 2003.
36. Entesarian M, Matsson H, Klar J, Bergendal B, Olson L, Arakaki R, Hayashi Y, Ohuchi H, Falahat B, Bolstad AI, Jonsson R, Wahren-Herlenius M, Dahl N. Mutations in the gene encoding fibroblast growth factor 10 are associated with aplasia of lacrimal and salivary glands. Nat Genet 37:125–127, 2005.
37. Jaskoll T, Abichaker G, Witcher D, Sala FG, Bellusci S, Hajihosseini MK, Melnick M. FGF10/FGFR2b signaling plays essential roles during in vivo embryonic submandibular salivary gland morphogenesis. BMC Dev Biol 5:11, 2005.
38. Steinberg Z, Myers C, Heim VM, Lathrop CA, Rebustini IT, Stewart JS, Larsen M, Hoffman MP. FGFR2b signaling regulates ex vivo submandibular gland epithelial cell proliferation and branching morphogenesis. Development 132:1223–1234, 2005.
39. Patel VN, Rebustini IT, Hoffman MP. Salivary gland branching morphogenesis. Differentiation 74:349–364, 2006.
40. Patel VN, Likar KM, Zisman-Rozen S, Cowherd SN, Lassiter KS, Sher I, Yates EA, Turnbull JE, Ron D, Hoffman MP. Specific heparan sulfate structures modulate FGF10-mediated submandibular gland epithelial morphogenesis and differentiation. J Biol Chem 283:9308–9317, 2008.
41. Bhushan A, Itoh N, Kato S, Thiery JP, Czernichow P, Bellusci S, Scharfmann R. Fgf10 is essential for maintaining the proliferative capacity of epithelial progenitor cells during early pancreatic organogenesis. Development 128:5109–5117, 2001.
42. Edlund H. Factors controlling pancreatic cell differentiation and function. Diabetologia 44:1071–1079, 2001.
43. Miralles F, Czernichow P, Ozaki K, Itoh N, Scharfmann R. Signaling through fibroblast growth factor receptor 2b plays a key role in the development of the exocrine pancreas. Proc Natl Acad Sci U S A 96: 6267–6272, 1999.
44. Elghazi L, Cras-Meneur C, Czernichow P, Scharfmann R. Role for FGFR2IIIb-mediated signals in controlling pancreatic endocrine progenitor cell proliferation. Proc Natl Acad Sci U S A 99:3884–3889, 2002.
45. Shen C-N, Marguerie A, Chien C-Y, Dickson C, Slack JM, Tosh D. All-trans retinoic acid suppresses exocrine differentiation and branching morphogenesis in the embryonic pancreas. Differentiation 75:62–74, 2007.
46. Hesselton RM, Greiner DL, Mordes JP, Rajan TV, Sullivan JL, Shultz LD. High levels of human peripheral blood mononuclear cell engraftment and enhanced susceptibility to human immunodeficiency virus type 1 infection in NOD/LtSz-scid/scid mice. J Infect Dis 172: 974–982, 1995.
47. Shultz LD, Schweitzer PA, Christianson SW, Gott B, Schweitzer IB, Tennent B, McKenna S, Mobraaten L, Rajan TV, Greiner DL. Multiple defects in innate and adaptive immunologic function in NOD/LtSz-scid mice. J Immunol 154:180–191, 1995.
48. Carlsson R, Martensson C, Kalliomaki S, Ohlin M, Borrebaeck CA. Human peripheral blood lymphocytes transplanted into SCID mice constitute an in vivo culture system exhibiting several parameters found in a normal humoral immune response and are a source of immunocytes for the production of human monoclonal antibodies. J Immunol 148: 1065–1071, 1992.
49. Duchosal MA, Eming SA, Fischer P, Leturcq D, Barbas CF 3rd, McConahey PJ, Caothien RH, Thornton GB, Dixon FJ, Burton DR. Immunization of hu-PBL-SCID mice and the rescue of human monoclonal Fab fragments through combinatorial libraries. Nature 355:258–262, 1992.
50. Ito M, Kobayashi K, Nakahata T. NOD/Shi-scid IL2rgamma (null) (NOG) mice more appropriate for humanized mouse models. Curr Top Microbiol Immunol 324:53–76, 2008.
51. Valujskikh A, Heeger PS. $CD4^+$ T cells responsive through the indirect pathway can mediate skin graft rejection in the absence of interferon-gamma. Transplantation 69:1016–1019, 2000.